INSTITUTE OF PHYSICS PUBLISHING JOURNAL OF OPTICS A: PURE AND APPLIED OPTICS

J. Opt. A: Pure Appl. Opt. **5** (2003) S518–S523 PII: S1464-4258(03)63005-9

Interactions in large arrays of solitons in photorefractive crystals

D Träger[1], A Strinić[2], J Schröder[1], C Denz[1], M Belić[2], M Petrović[2], S Matern[1] and H G Purwins[1]

[1] Institute of Applied Physics, Westfälische Wilhelms-Universität Münster, Corrensstraße 2/4, D-48149 Münster, Germany
[2] Institute of Physics, PO Box 57, 11001 Belgrade, Serbia

Received 1 May 2003, accepted for publication 9 July 2003
Published 27 October 2003
Online at stacks.iop.org/JOptA/5/S518

Abstract
Large two-dimensional spatial soliton arrays are generated experimentally and numerically in photorefractive media and their waveguiding properties at red and infrared wavelengths are demonstrated. An enhanced stability of solitonic lattices is achieved by exploiting the anisotropy of coherent soliton interaction and by controlling the relative phase between soliton rows. Manipulation of individual solitonic channels is accomplished by the use of separate control beams.

Keywords: Spatial solitons, solitonic lattices, waveguiding, pixel control

1. Introduction

When a wide Gaussian beam is launched in a photorefractive (PR) crystal in the self-focusing regime, it tends to break into a spatially disordered array of filaments, owing to the transverse modulational instability [1]. If, however, one launches an ordered array of Gaussian beamlets in conditions appropriate to the generation of spatial screening solitons [2], a much more stable solitonic lattice can be formed. Weakly interacting pixel-like arrangements of solitons that can be individually addressed are interesting for self-adaptive waveguiding [3, 4]. Furthermore, such lattices present natural examples of self-produced reconfigurable two-dimensional photonic crystals, although on a much larger scale.

Adaptive waveguides are of particular interest in all-optical information processing for their potential to generate large arrays, as well as for allowing many configurations with different interconnection possibilities. Spatial optical solitons are natural candidates for such applications, owing to their ability for self-adjustable waveguiding and versatile interaction capabilities, as demonstrated in light-induced Y and X couplers and beamsplitters, directional couplers and waveguides. In addition to such few-beam configurations, the geometries with many solitons propagating in parallel—the so-called soliton pixels, arrays or lattices—have been suggested for applications in information processing and image reconstruction [5–8]. Recently several groups demonstrated that quadratic arrays of spatial solitons can be formed in parametric amplifiers [8, 9] or in PR media for coherent [7, 10] and incoherent [4] beams.

In this paper we combine the features of spatial PR solitons to form pixel-like lattices with their waveguiding features, to realize waveguiding in large arrays of solitons at red and infrared wavelengths. We demonstrate how to achieve improved stability of solitonic lattices by utilizing anisotropic interaction between solitons, in particular the phase-dependent interaction between solitonic rows. We show how to manipulate individual or pairs of solitons in the lattice by the use of steering control beams. Here we will not address the photonic crystal aspects of the solitonic lattices, such as the existence and properties of the photonic bandgap, or the influence of lattice defects on the waveguiding behaviour.

To create two-dimensional lattices of solitons, the conditions for stable non-interacting propagation need to be defined. A crucial point in the parallel propagation of PR spatial solitons is their anisotropic mutual interaction [11]. Because the refractive index modulation induced by a single soliton reaches beyond its effective waveguide, phase-dependent coherent, as well as separation-dependent incoherent, interactions, such as repulsion, attraction or fusion, may appear between the neighbouring array elements. These interactions also affect the waveguiding characteristics of an individual solitonic channel. The separation between solitons and their nearest-neighbour (NN) arrangement, determined by the form of the lattice, must therefore be chosen carefully so as to minimize all forms of interaction. In our experiments, as well as numerical simulations, we determine the critical soliton distances for the given crystal thickness at which the

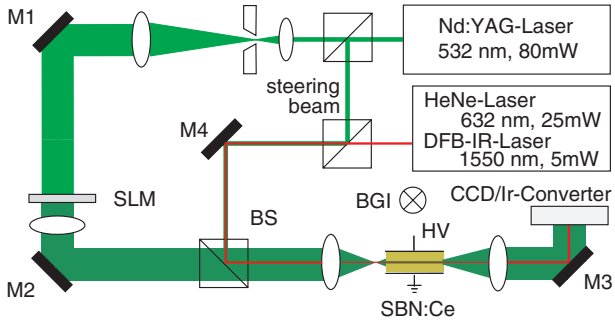

Figure 1. Experimental set-up for the creation, waveguiding and control of soliton lattices in a SBN:Ce crystal.
(This figure is in colour only in the electronic version)

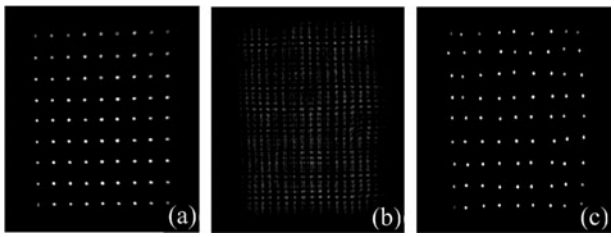

Figure 2. Stable propagation for 20 mm of a 9 × 9 rectangular lattice, with the pixel width 20 μm and separation $\Delta x = 110$ μm, $\Delta y = 125$ μm. Electro-optic coefficient 200 pm V^{-1}, external field 1 kV cm^{-1}. (a) Front crystal face. (b) Interference pattern on the back crystal face, without nonlinearity. (c) Back crystal face, with the nonlinearity turned on. The contrast in (b) is enhanced to see the structure.

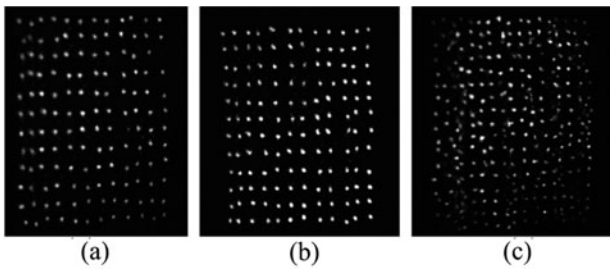

Figure 3. Interaction of solitons in a rectangular lattice for separations at or smaller than the critical distance after 20 mm propagation. (a) 12 × 12 array with $\Delta x = 80$ μm, $\Delta y = 95$ μm. (b) 12 × 12 array with $\Delta x = 70$ μm, $\Delta y = 85$ μm. (c) 17 × 17 array with $\Delta x = 60$ μm, $\Delta y = 75$ μm. Other parameters are as in figure 2.

interaction becomes noticeable. To achieve a closer packing of solitons, while maintaining propagation without interaction, the phase relationship between different beams in the array is exploited.

The layout of the paper is as follows. Section 2 displays the experimental set-up and presents results concerning the creation of different solitonic lattices and the waveguiding at different wavelengths. Section 3 introduces our numerical procedure, depicts the use of anisotropic interaction and phase relations between solitons to enhance the stability of the lattices and demonstrates the utilization of a steering beam for pixel control. Section 4 offers conclusions.

2. Experiment

2.1. Set-up

For the creation of soliton lattices and testing their waveguiding properties, the experimental set-up from figure 1 is used. A laser beam derived from a frequency-doubled Nd:YAG laser emitting at 532 nm illuminates a spatial light modulator (SLM), which imprints the image of a spot array onto the beam. The SLM in turn is imaged onto the front face of a PR SBN60:Ce crystal (5 mm × 5 mm × 20 mm), which is positioned so that the propagation direction is along the 20 mm axis. To exploit the dominant electro-optic component $r_{33} \approx 200$ pm V^{-1} of our SBN sample, the incident laser beam is linearly polarized parallel to the c axis of the crystal, perpendicular to the propagation direction. Regular patterns of up to 25 × 25 spots, each with a diameter of about 20 μm and an intensity of 110 nW, are imaged onto the front face of the crystal. In the linear regime—without an applied field—the beams diffract on their way through the crystal and display typical interference patterns. Applying an external DC electric field of about 1 kV cm^{-1} across the crystal and illuminating the crystal with uniform white light to induce an artificial dark conductivity creates appropriate conditions for the formation of spatial screening solitons and the self-focused soliton lattices appear. To probe the waveguiding properties of soliton lattices, additional optical paths for the probe and the control beam are provided in the set-up from figure 1. It should be noted that even larger lattices can be created without difficulty. The size is limited only by the size and uniformity of the crystal and the resolution of the imaging optical elements.

2.2. Lattices

Propagation without mutual interaction requires a sufficient initial distance between beams (figure 2). It also depends on other parameters influencing the soliton formation and propagation—initial beam profiles and phases, and the strength of the nonlinearity—but less crucially. A distance smaller than the critical distance for coherent interaction between the solitons leads to their attraction and eventual fusion. The attractive interaction is more pronounced in the y-transverse direction, perpendicular to the direction of the external field. For a given propagation distance this is reflected in the deformed appearance of the lattice. Lattice deformations are also caused by the crystal inhomogeneities that cannot be controlled. Hence the determination of the critical distance is qualitative, based on the inspection of series of runs with decreasing inter-soliton distances. A typical series of runs is depicted in figure 3, where the distance is reduced by increasing the density of packing of solitons. An estimate of the critical distance is found to lie between 3 and 4 beam diameters for our experimental conditions. This estimate is corroborated by numerical simulations.

It is our experience that large arrays of solitons can easily be formed in PR crystals. The larger the array the less significant the finite size (edge) effects. The number of pixels is mainly limited by the aperture of the PR crystal and the resolution of the inducing SLM. One can tailor the arrangement of beams according to specific needs. Examples of different non-interacting soliton arrays that were produced experimentally are shown in figure 4. Within our measurement

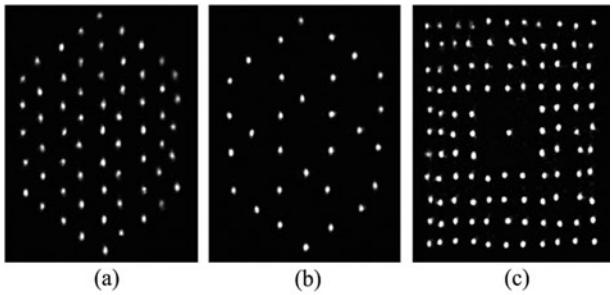

Figure 4. Examples of different experimental photonic lattices with pixel separations above critical, propagated for 20 mm. (a) Hexagonal, (b) honeycomb, (c) rectangular with an isolated central waveguide. Experimental parameters are as in figure 2.

technique we could not observe any coupling of neighbouring channels in such lattices. Based on the dynamic range of our imaging system this means that the signal-to-noise ratio (SNR) between adjacent solitonic channels is below 0.35%, or better than -2.5 dB. In larger arrays several applications of parallel soliton and waveguide formation can be envisioned. As an example, consider images consisting of large arrays of pixel spots arranged on a square lattice. In the linear regime an image can be reconstructed in a range that is limited by the depth of focus of the imaging optics, due to the blurring effects of diffraction. However, if these arrays of spots are propagating in the nonlinear, solitonic regime, the range of focus depth is enlarged to the length of soliton formation, i.e. to the length of the nonlinear crystal [8].

2.3. Waveguiding

Since a local change in the refractive index of the material is responsible for the creation of PR solitons, it is possible to probe this index modulation using beams at different wavelengths. Such a possibility is especially useful for all-optical telecommunications applications, where light beams are used to create and manipulate waveguides. The interesting point in using other wavelengths is that one may guide light that is not sensitive to photorefraction and does not exhibit any self-focusing or soliton-forming characteristics. In our Ce-doped SBN sample no PR effect was noticed at red or infrared wavelengths for the laser intensities used in the experiments.

To test the waveguiding properties of single channels of our solitonic arrays, the wavelength selectivity of the PR effect in SBN:Ce crystal is exploited, to scan the array with an intense probe beam at different wavelengths without destroying the original channels. Two probes are utilized, as shown in figure 1. One probe is derived from a HeNe laser radiating at 633 nm and the beam is positioned successively to the positions of previously induced solitons in the crystal. We find the probe beam to be guided by each of the solitonic channels individually. A scan of the rectangular array with the red probe is shown in figure 5. Every single channel is scanned separately, and the individual images are superimposed electronically. Coupling efficiency for the amount of energy coupled into a single waveguide is measured to be around 56% [3]. Apparently the radiated light is not trapped by the adjacent channels.

The other probe is derived from the commercial fibre-coupled DFB laser emitting at the infrared telecommunications

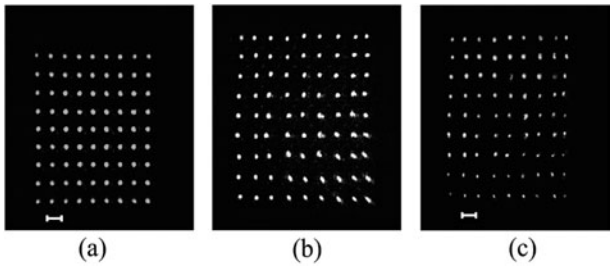

Figure 5. Probing a solitonic array for waveguiding in separate channels, with an overlapping probe beam at 633 nm. (a) Initial 9×9 array with $\Delta x = 100$ μm, $\Delta y = 115$ μm. (b) Propagated array without probe. (c) Probed array. The bar in (a) and (c) equals 100 μm. Other parameters are as in figure 2.

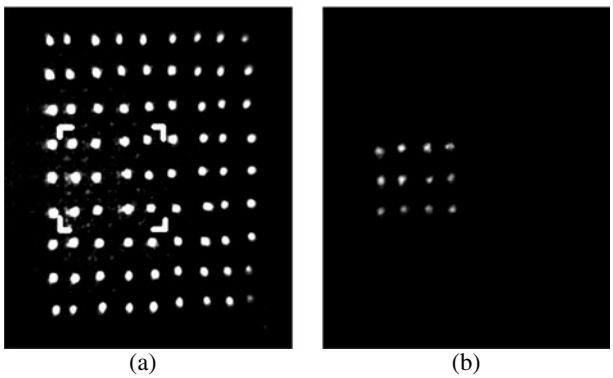

Figure 6. Probing an array for waveguiding with a probe beam at 1.55 μm. (a) Propagated 9×9 array with $\Delta x = 80$ μm, $\Delta y = 95$ μm. The marked section of the array is probed. (b) Probed section, visualized with an infrared-to-visible light converter. Other parameters are as in figure 2.

wavelength of 1550 nm. The imaging optics used in the experimental set-up now had to be modified. To visualize the infrared waveguiding it was necessary to use an infrared-to-visible converter [12, 13]. This consists of a dc-operated planar semiconductor-gas discharge system that is sensitive to a wide range of IR wavelengths (0.8–11 μm). The spectral range of its sensitivity is determined by the material of the high resistance semiconductor. In the present work a GaAs:Cr detector is used, which covers the range from 0.8–1.7 μm. An incoming IR irradiation distribution increases the conductivity of the semiconductor, due to the intrinsic photoeffect. Hence the operation of the gas discharge shifts to a higher current density, which leads to a two-dimensional brightness distribution of the gas discharge glow, thus permitting the system to emit in the visible. It was used in the reflection configuration in our experiments, allowing us to simultaneously observe the green light from the soliton creation and the infrared output.

Again, the 9×9 lattice of solitons is scanned channel by channel with the infrared beam and single images are added electronically. In figure 6 a region of 4×3 guided beams is shown as an example. The red or infrared light do not produce any nonlinear effects in the crystal on their own. This is checked by removing the refractive index modulation of the lattice, using strong white light illumination. In the absence of a lattice, the red and infrared beams exhibit linear propagation in the crystal.

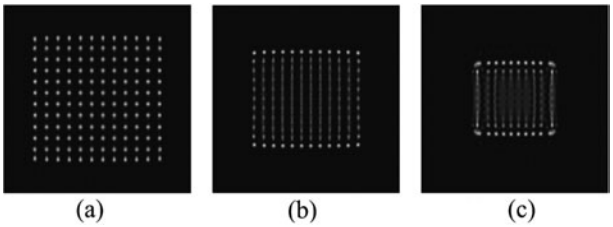

Figure 7. Numerical simulation of a square 12 × 12 soliton in-phase lattice after 20 mm propagation, with an electro-optic coefficient of 210 pm V^{-1} and an electric field of 900 V cm^{-1}. The total size of data windows is 1 mm^2 and the initial FWHM size of individual beams is 20 μm. (a) $\Delta x = \Delta y = 60$ μm. (b) $\Delta x = \Delta y = 50$ μm. (c) $\Delta x = \Delta y = 40$ μm.

3. Numerics

3.1. Numerical lattices

Numerical simulations are based on the paraxial wave equation describing the anisotropic propagation of coherent optical beams in saturable PR media:

$$2ikn_0\partial_z A + \nabla_\perp^2 A = -k^2 n_0^4 r_{33}(\partial_x \phi)A, \qquad (1)$$

where k is the wavenumber in vacuum, $n_0 \approx 2.35$ is the bulk refractive index, $\nabla_\perp^2$ is the transverse Laplacian and A is the slowly varying envelope of the electric field of the light. The paraxial equation is augmented with the equation for the electrostatic potential $-\nabla\phi = \mathbf{E}$ of the space-charge field $\mathbf{E}$ generated in the crystal [14, 15]:

$$\nabla^2\phi + \nabla\phi \cdot \nabla \ln(1 + I) = E_e \partial_x \ln(1 + I), \qquad (2)$$

where E_e is the external field. The light intensity I is normalized to the background intensity. These equations are solved together, in the manner described in [16]. Behaviour similar to that in the experiment was found: parallel propagation of coherent solitons with varying separation can be adjusted to be almost without interaction (figure 7 (a)) whereas for separations below the critical length the fusion of soliton columns is observed (figures 7(b) and (c)).

Propagation of incoherent lattices is found to be more stable than the propagation of coherent in-phase lattices for identical conditions. However, our intention is to exploit the possibility of using the distribution of phase across the lattice in coherent interaction to achieve closer packing while maintaining propagation without interaction. The comparison for different lattices is provided in figure 8. One can think of different phase distributions to stabilize different lattices. We find that the best overall results are obtained when the adjacent rows of solitons are out-of-phase. This is easily accomplished in the square lattice and is a bit more difficult in the hexagonal and honeycomb lattices. It is also in agreement with the theoretical expectations of the anisotropic interaction: along rows the solitons are in-phase and along columns they are out-of-phase, which makes the interaction between them universally repulsive and leads to enhanced stability.

3.2. Phase engineering

To test the idea of using phase engineering for enhancing the stability of arrays of solitons, different lattices were formed and propagated (figure 8). The NN separation in figure 8 for all lattices is 60 μm, which is about 3/4 of the critical distance from figure 3 and three times the FHWM of the initial beams. It is seen that the in-phase lattices deform fast and that, after 40 mm of propagation, owing to the attractive forces along the y direction, some rows are lost in the quadratic lattice, while the hexagonal and honeycomb lattices are strongly deformed. The honeycomb lattice deforms continually from the direct to the inverse (hexagonal) lattice and back (figures 8(f) and (i)). However, out-of-phase lattices for identical initial conditions and at the same propagation distance are only slightly deformed. In all the cases the phase engineered lattices were the most stable. It is also visible that the edge effects decrease with increasing lattice size. We are in the process of investigating the cross-talk and coherence effects between neighbouring pixels that the reduction in separation and phase engineering may have brought about.

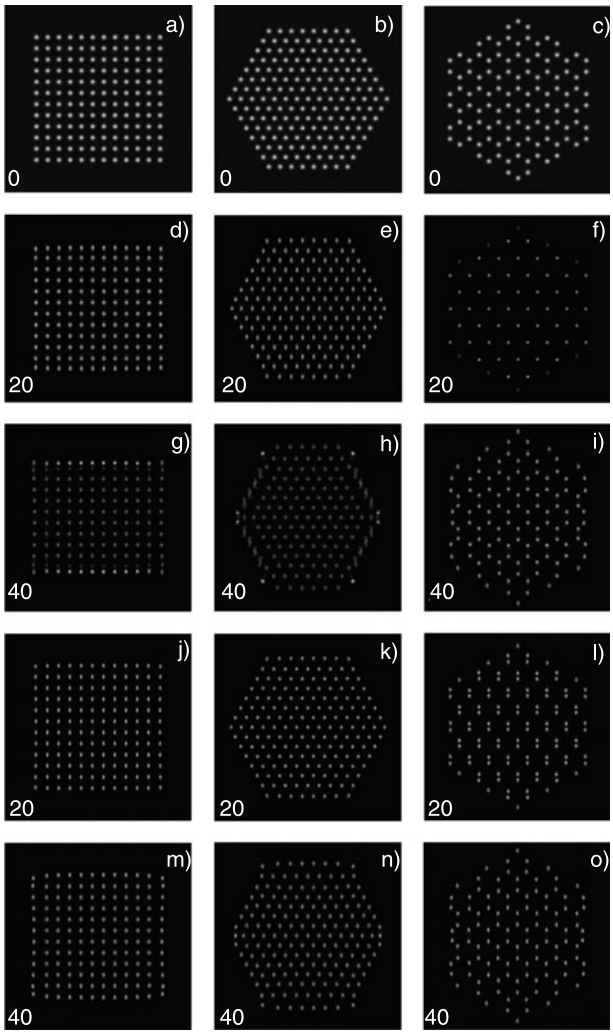

Figure 8. Square, hexagonal and honeycomb soliton lattices with 60 μm NN separation, propagated for 40 mm numerically. (a)–(c) Initial intensity distributions. (d)–(f) In-phase lattices propagated for 20 mm. Note in (f) the inversion of the honeycomb lattice. (g)–(i) In-phase lattices propagated for 40 mm. Strong edge deformation is evident. (j)–(o) The same lattices, but with alternate rows of solitons out-of-phase, propagated for 20 and 40 mm. Other data as in figure 7.

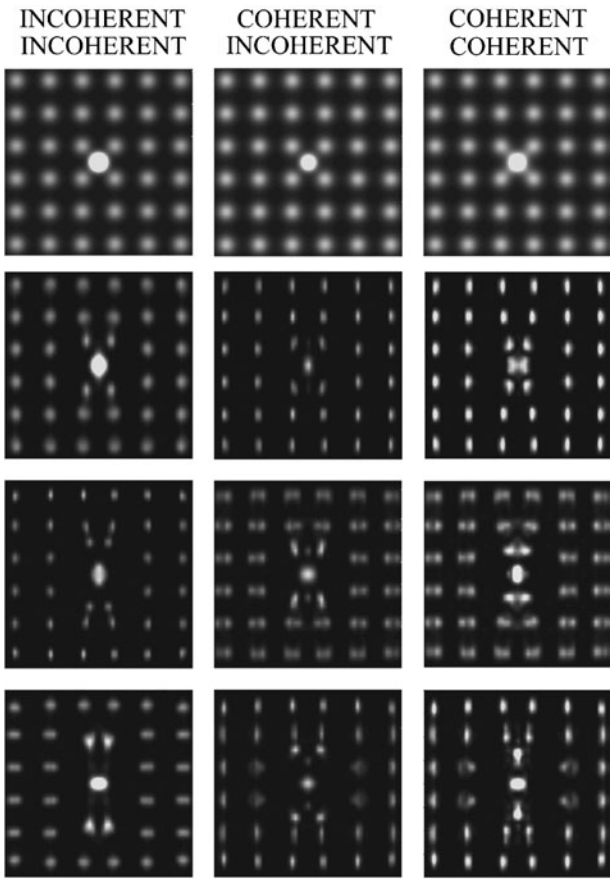

Figure 9. Illustrating the action of a phase-sensitive control beam on individual solitons in a square lattice. In the left column both the lattice and the control beam are incoherent, in the middle column the lattice is coherent whereas the control beam is incoherent, and in the right column both the lattice and the control are coherent. In the left column the initial intensity of the control beam is seven times the intensity of any pixel, as in [4], while in the other two columns it is three times the pixel intensity. Also, the coupling strength in the left column is $\Gamma = 13$, and in the other two $\Gamma = 10.5$. The first row represents the initial intensity distribution, while the second, third and fourth rows are after 15, 20 and 25 mm of propagation, respectively.

3.3. Pixel control

To use solitonic arrays for applications in information technology it is highly desirable to have a means of manipulating individual waveguides in order to combine different channels, separate them or induce energy exchange between them. For this purpose the well-known interaction effects of spatial PR solitons can be exploited [7, 11]. We utilize here a supplementary control beam derived from the Nd:YAG laser that can be focused anywhere on the front face of the crystal (the steering beam in figure 1). Varying the phase of the control beam relative to the phase of the array elements, a phase-sensitive coherent or incoherent interaction can be induced, that may lead to fusion or repulsion of different solitons in the array. Early experimental results for an incoherent control were presented in [4, 7, 10]. Here we display the influence of a phase-sensitive control beam obtained numerically, using experimental data from [4].

The cases of incoherent and coherent control beams relative to the lattice are presented in figure 9. Also, the lattice itself is, in one case, incoherent and in the other case, coherent. The left column in figure 9 corresponds to an experiment performed in [4] and the simulation seems to closely resemble the experimental result. However, our interpretation is different from the one offered in [4]. Whereas the authors report seeing only attraction of the nearest lattice pixels toward the control beam, we see that they are attracted in the x direction but repulsed in the y direction. In addition, a portion of the four pixels is focused in the centre. It seems to us that this interpretation is consistent with the experimental figure 4 in [4]. Such an interpretation is also consistent with the intricacies of the anisotropic interaction between solitons where, in addition to attraction, repulsive forces are seen as well. Similar tendencies, but different in detail, are visible in the middle and right columns in figure 9.

4. Conclusions

In conclusion, we have discussed several aspects of the interaction of solitons in large arrays, to be utilized in all-optical waveguides and interconnects. Different stable lattices of solitons are produced experimentally in a SBN:Ce crystal that may find use in all-optical information processing. We have displayed the formation of two-dimensional arrays of solitons that are able to guide light at different wavelengths, in particular at 633 and 1550 nm. We have simulated solitonic lattices numerically by solving the paraxial propagation equation for self-focusing beams in PR crystals, together with the equation for the electric potential of the space-charge field. Enhanced stability of these lattices is achieved by the phase engineering of soliton rows. Different distributions of phase across a coherent lattice are used to achieve closer packing while maintaining minimal interaction between pixels. The best results are obtained when the adjacent rows of solitons are out-of-phase. We have shown how to use a supplementary steering beam to manipulate selected channels in the solitonic lattice.

Acknowledgments

AS and MB gratefully acknowledge financial support from the Alexander von Humboldt Foundation, for the stay and work at WWU Münster. DT acknowledges support from the Konrad-Adenauer-Stiftung. Part of this work was supported by the Deutsche Forschungsgemeinschaft. Work at the Institute of Physics is supported by the Ministry of Science, Technologies, and Development of the Republic of Serbia, under projects OI 1475 and 1478. We thank Dr Juergen Petter, Institut für Angewandte Physik, TU Darmstadt, for help in the experiment on waveguiding.

References

[1] Mamaev A V, Saffman M, Anderson D Z and Zozulya A A 1996 *Phys. Rev.* A **54** 870
[2] For an overview see the Special Issue on solitons, Segev M (ed) 2002 *Opt. Photonics News* **13**
[3] Petter J and Denz C 2002 *J. Opt. Soc. Am.* B **19** 1145

[4] Chen Z and McCarthy K 2002 *Opt. Lett.* **27** 2019
[5] Mamyshev P V, Bosshard C and Stegeman G I 1994 *J. Opt. Soc. Am.* B **11** 1254
[6] Krolikowski W and Kivshar Yu S 1996 *J. Opt. Soc. Am.* B **13** 24
[7] Weilnau C, Ahles M, Petter J, Träger D, Schröder J and Denz C 2002 *Ann. Phys., Lpz.* **9** 1
[8] Bramati A, Chinaglia W, Minardi S and Trapani P Di 2001 *Opt. Lett.* **26** 1409
[9] Minardi S, Sapone S, Chinaglia W, Trapani P Di and Berzanskis A 2000 *Opt. Lett.* **25** 326
[10] Petter J, Schröder J, Träger D and Denz C 2003 *Opt. Lett.* **28** 438
[11] Krolikowski W, Saffman M, Luther-Davies B and Denz C 1998 *Phys. Rev. Lett.* **80** 3240
[12] Matern S, Marchenko V M, Astrov Yu A, Portsel L M and Purwins H G 2002 *Proc. SPIE* **4669** 13
[13] Astrov Yu A, Egorov V V, Kasymov Sh S, Murugov V M, Paritsky L G, Ryvkin S M and Sheremetiev Yu N 1977 *Kvant. Elektron.* **4** 1681
[14] Zozulya A A and Anderson D Z 1995 *Phys. Rev.* A **51** 1520
[15] Belić M R, Vujić D, Stepken A, Kaiser F, Calvo G F, Agullo-Lopez F and Carrascosa M 2002 *Phys. Rev.* E **65** 066610
[16] Stepken A, Kaiser F and Belić M R 2000 *J. Opt. Soc. Am.* B **17** 67